Journal of Applied Sciences

ISSN 1812-5654

science alert

ANSInet
an open access publisher
http://ansinet.com

Journal of Applied Sciences 8 (18): 3191-3198, 2008
ISSN 1812-5654

Nickel(II) Complexes with Sulphonylhydrazone Derivatives: Spectroscopic and Electrochemical Studies

[1]A. Reguig, [2]M.M. Mostafa, [1]L. Larabi and [1]Y. Harek
[1]Département de Chimie, Faculté des Sciences, Université Abou Bakr Belkaid, Tlemcen, Algérie
[2]Department of Chemistry, Faculty of Science, Mansoura University, Mansoura, Egypt

Abstract: The synthesis and characterization of benzene and p-toluenesulfonylhydrazones derived from salicylaldehyde and 2-hydroxyl-1-naphthaldehyde and their Ni(II) complexes are reported. The structural investigation of these compounds was based on elemental analysis, magnetic moment and spectral (ultraviolet, infrared and ^{1}H-NMR). The Ni(II) complexes were diamagnetic. The stoichiometry of all the complexes was found to be 1:2 and the geometry around the nickel ions is square planar. The electrochemical behavior of the Ni(II) complexes was investigated in DMSO by cyclic voltammetry (CV), rotating disc electrode (RDE) and coulometry. The complexes displayed Ni(III)/Ni(II) couples irreversible waves and the substitution of the phenyl by naphthyl fragments causes a negative shift in the formal potential.

Key words: Sulphonylhydrazone, Ni(II) complex, cyclic voltammetry, rotating disc electrode

INTRODUCTION

It is known that the transition metal complexes play a central role in the conduction of molecular materials, which display unusual conducting and magnetic properties and find applicability in material chemistry, supramolecular and biochemistry (Chandra and Kumar, 2004, 2005; Chandra *et al*., 2006). The hydrazone derivatives as ligands for transition metal ions constitute an important class of ligands which have been extensively studied in coordination chemistry mainly due to their facile synthesis, their photochromic effect (Wong and Bruscato, 1968; Zady *et al*., 1975; Jacques, 1984; Becker and Chagneau, 1992; Bulanov *et al*., 2002; Hadjoudis and Mavridis, 2004), their physico-chemical properties and application in many important chemical process that include sensors, non-linear optics, medicine and others (Armstrong *et al*., 2003; Schmitt *et al*., 2003; Bakir *et al*., 2004). It is well established that transition metals are readily susceptible to oxidation and reduction because of their ability to easily change oxidation states. Thus, the high oxidation state transition metal complexes are well known to be biologically important and interesting because of their redox enzymes properties (Margerum *et al*., 1975; Bour *et al*., 1971; Ruiz *et al*., 1997; Cervera *et al*., 1998).

The redox properties include oxidation of the central metal ion with ligands have been previously studied and reported by Larabi *et al*. (2003). The redox potential of the Cu(II)/Cu(III) and Ni(II)/Ni(III) complexes have been shown to be markedly affected by the nature of the chelating ligand with the complexes (Larabi *et al*., 2003; Schmidt and Chmielewski, 2003).

In earlier research (Larabi *et al*., 2003) salicylaldehyde benzenesulphonyl-hydrazone (SBSH), naphthaldehyde benzenesulphonylhydrazone (NBSH), salicylaldehyde p-toluene-sulphonylhydrazone (STSH) and naphthaldehyde p-toluenesulphonyl-hydrazone (NSTH) (Scheme 1) were synthesized and the structures of their Cu(II) complexes were reported. The present study is concerned with the elucidation of these ligands structures by the use of spectroscopic methods (UV, IR and ^{1}H-NMR). In addition, information about the stereochemistry of their Ni(II) complexes has been obtained from spectral measurements. It is worthwhile to note that little attention on the electrochemical behavior of metal complexes derived from hydrazone derivatives was given. In order to contribute in this area, it is studied extensively the electrochemical properties of the Ni(III)/Ni(II) couple, which was affected by the donor environments. So, the present study is also to investigate the capacity of the chelating ligands under investigation to stabilize nickel(III) complexes and to elucidate the mechanism of the oxidation process by means cyclic voltammetry, rotating disc electrode and bulk electrolysis techniques.

Corresponding Author: L. Larabi, Département de Chimie, Faculté des Sciences, Université Abou Bakr Belkaid, Tlemcen, Algérie, Tel: 0021343381018 Fax: 0021343286308

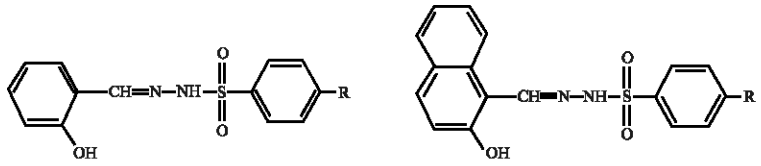

SBSH (H_2L_1): R =H
STSH (H_2L_3): R =CH_3

NBSH (H_2L_2): R = H
NTSH (H_2L_4): R = CH_3

Scheme 1: Presentation of the ligands

MATERIALS AND METHODS

All the chemicals used for the preparation of the ligands were of BDH quality. Conductivity measurements were carried out in DMF (ca. 10^{-3} mol L^{-1}) using a Tacussel conductivity bridge model 75. Magnetic susceptibilities were determined using a Johnson Matthey balance at room temperature (25°C) with $Hg[Co(SCN)_4]$ as standard. Perkin-Elmer PE 938 and Pye Unicam model SP. 3-300 spectrophotometers were used to record the IR spectra using KBr pellets and as Nujol mulls between CsI plates. UV-visible spectra were recorded in Nujol, in acetone and chloroform on a Perkin-Elmer model 550-S spectrometer. ^{1}H-NMR spectra were recorded using Bruker Ac 200 spectrophotometer at Strasbourg University (France). Elemental analysis were carried out in the Micro-analytical unit at Cairo University (Egypt). The electrochemical experiments were carried out using a Trace-lab50 from Radiometer which includes a polarographic analyzer (Pol 150), a polarographic stand (MDE 150) and trace Master 5 software. Cyclic voltammetry was performed using a conventional three electrodes system. The working electrode was a pre-polished glassy carbon (GC) disc of 3 mm diameter (Radiometer). Potentials are expressed versus the Ag/AgCl (KCl 3 mol L^{-1}) electrode separated from the test solution by a salt bridge containing the solvent/supporting electrolyte. The auxiliary electrode was a platinum wire. The RDE study was performed using Radiometer model BM-EDI101 rotating disc electrode. The rotating speed ω was regulated by an Asservitex model CTV101 from the Radiometer.

The following solutions were studied: 0.5, 1.0, 1.5, 2.0, 3.0, 3.5, 4.0 and 4.5 mmol L^{-1} of complexes in DMSO and 0.1 mol L^{-1} $N(Et)_4ClO_4$ as supporting electrolyte.

Caution: $N(Et)_4ClO_4$ is sensitive to shock or heat. The RDE voltammograms were recorded in each solution, using a scan rate of 5 mV sec^{-1} and rotating speeds ω of 25, 50, 75, 100, 150, 200, 300 and 400 rpm. In The CV measurements, scan rate v of 10, 25, 50, 100, 200, 400, 500, 1000 and 2000 mV sec^{-1} were employed. All experiments were carried out at 25°C ±0.1 using a Julabo thermostat. In the coulometric experiments, the auxiliary electrode was separated from the solution by a glass frit disk and the working electrode was controlled by a Radiometer PGP201 potentiostat.

Synthesis of the ligands: Benzene and p-toluenesulphonylhydrazine (BSH, TSH) were prepared according to literature procedures (Vogel, 1989) and the ligands SBSH, NBSH, STSH and NTSH were synthesized as reported earlier (Larabi *et al*., 2003).

Synthesis of the complexes: The metal complexes were prepared using a general method. A hot absolute EtOH solution of Ni(II) acetate (1 mmol) was added to a hot solution of corresponding ligand (2 mmol) in EtOH with continuous stirring. The precipitated was filtered off hot, washed several times with an absolute EtOH and dried in a dessicator over silica gel.

RESULTS AND DISCUSSION

Structural studies: Analytical results and physical properties of the ligands and the product complexes are given in Table 1. They are air-stable, insoluble in most common organic solvents but easily soluble in DMF and DMSO. The molar conductivities of the complexes in DMF (25°C) are in the 3-7 ohm^{-1} cm^2 mol^{-1} range, indicating a non-electrolytic nature (Geary, 1971).

The position of the significant IR bands of all ligands (H_2L_1, H_2L_2, H_2L_3 and H_2L_4) and their nickel(II) complexes are summarized in Table 2. The IR spectra of H_2L_1 show two bands at 3020 and 2880 cm^{-1} assignable to γ_aOH and γ_sOH vibrations, respectively. These bands are observed at 3420 and 2920 cm^{-1} for H_2L_3. The existence of those bands at lower wave-numbers suggests the presence of intramolecular hydrogen bonding of the type (O-H....N) (Bullock and Tajmir-Riahi, 1978). Also, the spectra show strong band at 3160 for H_2L_1 and 3200 cm^{-1} for H_2L_3 assigned to γNH vibration. Moreover, the

Table 1: Colors, melting point, partial elemental analysis and molar conductivities of the metal complexes

Complex	Color	M.P. (°C)	% C found (Calcd.)	% H found (Calcd.)	% N found (Calcd.)	% Ni found (Calcd.)	Λ*m in DMF
$[Ni(HL_1)_2]$	Grass green	>260	51.1 (51.3)	3.6 (3.6)	9.2 (9.2)	9.2 (9.6)	7
$[Ni(HL_2)_2]$	Yellowish-green	>260	58.0 (57.6)	3.7 (3.7)	8.0 (7.9)	8.2 (8.3)	3
$[Ni(HL_3)_2]$	Yellowish-green	>260	52.8 (52.8)	4.0 (4.1)	8.8 (8.8)	9.0 (9.2)	5
$[Ni(HL_4)_2]$	Olive green	>260	58.7 (58.6)	4.3 (4.1)	7.6 (7.6)	7.6 (8.0)	3

*$\Omega^{-1}cm^2\ mol^{-1}$

Table 2: Infrared spectra of the ligands and their metal complexes

Compounds	ν (NH)	ν (C=N)	ν (OH)	ν (SO_2)	ν (Ni-N)	ν (Ni-O)
H_2L_1	3160	1620	3020 (free) 2880 (HB)	495	-	-
$[Ni(HL_1)_2]$	3160	1600	-	495	430	555
H_2L_2	3180	1630	3030 (free) 2880 (HB)	550	-	-
$[Ni(HL_2)_2]$	3180	1600	-	550	430	520
H_2L_3	3200	1610	3420 (free) 2920 (HB)	500	-	-
$[Ni(HL_3)_2]$	3200	1600	-	500	425	560
H_2L_4	3200	1625	3460 (free) 3040 (HB)	495	-	-
$[Ni(HL_4)_2$	3200	1600	-	495	430	525

HB: Hydrogen bonding, -: Absence of the bond

bands at ~1620, ~1430 and ~1270 cm^{-1} are assigned to γ (C=N), γ (C-O) and γOH vibrations, respectively. The four bands at ~1325, ~1170, ~570 and ~480 cm^{-1} are attributed to γ_sSO_2, $\gamma_{as}SO_2$, δSO_2, γSO_2 vibrations, respectively and remain more or less at the same positions as reported in literature (Bellamy, 1958). The observation of broad but weak bands in the 2000-1800 and 2400-2200 cm^{-1} regions suggests the existence of hydrogen bonding of the type N-H....N (intermolecular hydrogen bonding). The IR spectra of both ligands in $CHCl_3$ show the obscure of hydrogen bonding. The ^{1}H-NMR spectra of H_2L_1 and H_2L_2 in d_6-DMSO show two singlet signals at 11.50 and 11.10 ppm, downfield of TMS, with equal ratio and assigned to the protons of OH and NH groups, respectively. Those two signals disappear upon deuteration. The IR spectra of H_2L_2 and H_2L_4 show three important bands. H_2L_2 exhibits bands at 3180, 3030 and 2880 cm^{-1} while H_2L_4 show bands at 3200, 3460 and 3040 cm^{-1}. These bands can be assigned to γ_aOH γ_sOH and γNH vibrations, respectively. The position of the latter bands suggests that the OH group is strongly affected by strong intramolecular hydrogen bonding of the type O-H....N (Bullock and Tajmir-Riahi, 1978). In addition, the observation of broad weak bands in the 2000-1800 and 2400-2200 cm^{-1} regions is also taken as evidence for the presence of hydrogen bonding. The ^{1}H-NMR spectra of H_2L_3 and H_2L_4 in d_6-DMSO show three singlet signals at 2.4, 10.2 and 11.5 ppm, downfield of TMS, with ratio 3:1:1 and are assigned to the protons of CH_3, NH and OH groups, respectively. The latter two signals disappear upon deuteration. All these observations suggest the structures for the ligands given in Scheme 2.

The UV spectra of H_2L_1 and H_2L_3 in acetone show four bands. H_2L_1 exhibits the bands at 438, 370, 330 and 304 nm while H_2L_3 shows the bands at 430, 412, 380 and 340 nm. These bands are assigned to n→π* (SO_2), n→π* (C=N), π→π* (SO_2) and π→π* (C=N), respectively (Rao, 1975). On the other hand, the UV spectra of H_2L_2 and H_2L_4 in acetone show five bands. H_2L_2 shows bands at 450, 418, 376, 360 and 330 nm while H_2L_4 exhibits bands at 450, 438, 380, 360 and 328 nm. These bands may be assigned to n→π* (SO_2), n→π* (C=N), π→π* (SO_2) and π→π* (C=N) and π→π* (naphtyl), respectively (Rao, 1975). It is interesting to point that the above mentioned bands are split into two for each band in $CHCl_3$. This suggests that the ligands exist in two forms (free and hydrogen-bonded) upon dissolving in $CHCl_3$ as shown in Scheme 3.

In comparing the IR spectra of the Ni(II) complexes with the parent ligands (Table 2), we observed that the ligands behave more or less in the same way. The ligands coordinate in a bidentate manner via the azomethin group (C=N) and the OH (phenolic or naphtolic) groups forming six membered ring including the metal ions.

The displacement of a hydrogen atom from the OH group is proved as follows:

The pH drop and the conductance increase upon successive addition of ligand solution on titrating against Ni(II) acetate solution prove the liberation of ethanoic acid during complex formation. The spectral data (IR and ^{1}H-NMR) confirm participation of OH in bonding. Thus, the γOH disappears, the C=N band shifts to lower wave number and new bands appear in the 560-520 and 430-410 cm^{-1} regions assignable to γ(M-O) and γ(M-N) (Ferraro, 1971; Chandra *et al.*, 2005), respectively. The latter result supports the involvement of nitrogen in coordination. Finally the test of OH group by spot test technique (Feigl, 1982) is negative.

The diamagnetic behaviors as well as the observation of a broad band centered at ca. 476 nm assigned to $^1A_{1g}\rightarrow{}^1A_{2g}$ transition are evidences for square-planar geometry (Lever, 1968; Sacconi, 1966) around the nickel(II) ion. The disappearance of the OH proton and the existence of the NH proton in the ^{1}H-NMR spectra of the nickel complexes, prove the replacement of a hydrogen atom from the OH group only.

Electrochemical studies: The electrochemical behavior of all the Ni(II) complexes are similar in the same conditions and depends on the potential range. The cyclic

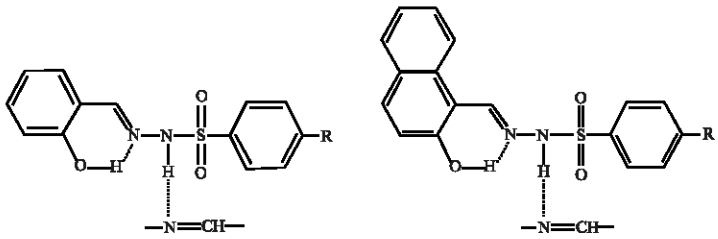

Scheme 2: Presentation of the inter- and intramolecular hydrogen bonding

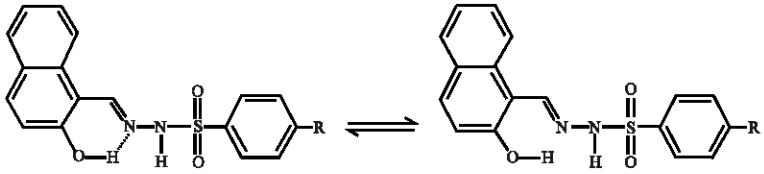

Scheme 3: Presentation of the two forms of the ligands

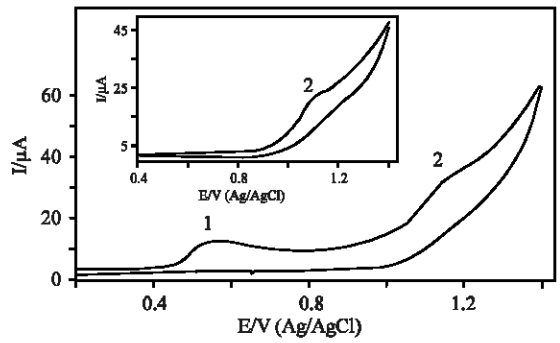

Fig. 1: Cyclic voltammogram of 1 mmol L^{-1} $[Ni(HL_1)_2]$ in DMSO-TEAP (0.1 mol L^{-1}) at GCE; scan rate 0.1 V sec^{-1} at 25°C. Inset shows the CV of H_2L_1 (1 mmol L^{-1}) in the same solution

voltammogram of 1 mmol L^{-1} $[Ni(HL_1)_2]$ which is similar to that of $[Ni(HL_3)_2]$, in DMSO with 0.1 mol L^{-1} $N(Et)_4ClO_4$ as the supporting electrolyte is shown in Fig. 1. The voltammogram obtained, in the anodic direction, at a glassy carbon electrode shows two prominent oxidation waves at E_{pa} values 0.58 V (peak 1) and 1.22 V (peak 2). It should be mentioned that the supporting electrolyte $N(Et)_4ClO_4$ in DMSO did not show any redox activity in the potential range studied. So The anodic process (peak 2) is a result of the redox process of the corresponding ligand (H_2L_1). This signal is also observed in the CV of H_2L_1 under similar conditions and may be attributed to the irreversible oxidation of the NH group. The other peak (peak 1) observed in the CV plot is assumed to be a result of the oxidation occurring at the Ni(II) ion. This redox couple studied in the interval of 10-2000 mV sec^{-1} shows a linear variation of I_{pa1} versus $\nu^{1/2}$ at complex concentrations ≤3 mmol L^{-1}. Moreover the slope $\Delta E/\Delta \log \nu$ has the value of 0.046 V that is larger those expected for reversible process. These suggests a diffusion controlled irreversible Ni(II)-Ni(III) process at complex concentrations ≤3 mmol L^{-1}. The value of the symmetry coefficient α was also determined using Eq. 1 (Nicholson and Shain, 1964) and was found to be 0.45 when n = 1, which confirmed the irreversible nature of the electrode process Ni(II)-Ni(III).

$$E_p - E_{p/2} = \frac{48\ mV}{\alpha n} \qquad (T = 25°C) \qquad (1)$$

where, $E_{p/2}$ is the half-peak potential, n is the total number of electrons involved in the reaction.

On the other hand, the Fig. 2 shows that at higher complex concentration and for ν>400 mV sec^{-1} the increase of I_{pa1} with $\nu^{1/2}$ was less than linear. These results indicate that the complex oxidation occurs via an irreversible electron transfer followed by a chemical reaction at complex concentrations >3 mmol L^{-1}.

We also carried out the RDE experiments for $[Ni(HL_1)_2]$ at different concentrations in DMSO solutions in order to elucidate the reaction mechanism. Figure 3 shows the results plotted according to Levich equation:

$$I_l = 0.620nFAD^{2/3}\nu^{-1/6}\omega^{1/2}C_0 \qquad (2)$$

where, D, ν, ω and C_0 are the diffusion coefficient, the kinematic viscosity, the rotation speed and the bulk concentration of the reactant in the solution respectively and all other parameters have their conventional meanings.

Levich equation predicts that the plot of I_l vs. $\omega^{1/2}$ should be linear. This was true only when the complex

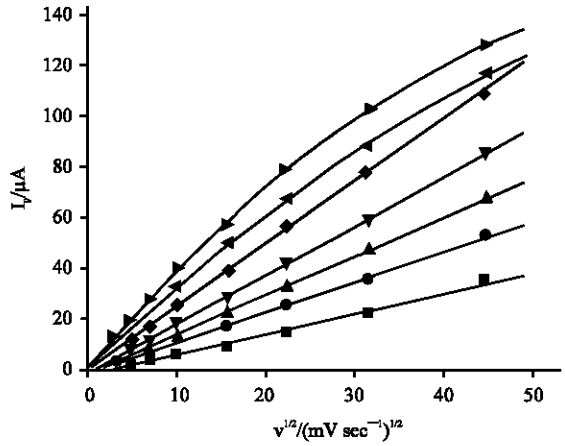

Fig. 2: Variation of the anodic peak currents, I_{pal}, versus $v^{1/2}$ for various $[Ni(HL_1)_2]$ concentrations: (■) 0.5; (●) 1.0; (▲) 1.5; (▼) 2.0; (◆) 3.0; (◄) 4.0 and (►) 4.5 mmol L^{-1}

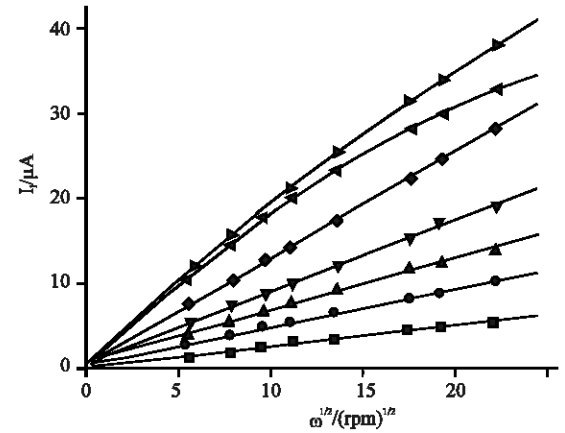

Fig. 3: Levich plots of the first anodic limiting current of $[Ni(HL_1)_2]$ at different concentrations: (■) 0.5; (●) 1.0; (▲) 1.5; (▼) 2; (◆) 3; (◄) 4.0 and (►) 4.5 mmol L^{-1} at a GCE; V=10 mV sec^{-1}

concentration was ≤3 mmol L^{-1} (Fig. 3), while for concentrations higher than 3 mmol L^{-1} the corresponding plots were found to be of curved shape. This result is an indication of a kinetic limitation (Razmi-Nerbin and Pournaghi-Azar, 2002).

The behavior of the oxidation peak currents (I_{pal}) of $[Ni(HL_3)_2]$ and the I_l vs. $\omega^{1/2}$ equations is identical to that reported for CV and RDE studies of $[Ni(HL_1)_2]$.

The cyclic voltammogram of $[Ni(HL_2)_2]$ at a glassy carbon electrode with DMSO as the solvent (Fig. 4) is very similar to that of $[Ni(HL_4)_2]$. The voltammogram obtained, in the anodic direction, displays three

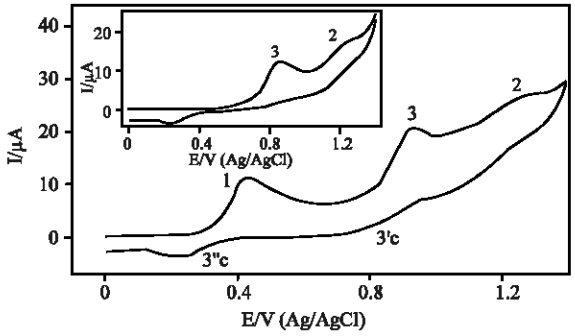

Fig. 4: Cyclic voltammogram of 1 mmol L^{-1} $[Ni(HL_2)_2]$ in DMSO-TEAP (0.1 mol L^{-1}) at GCE; scan rate 0.1 V sec^{-1} at 25°C. Inset shows the CV of H_2L_2 (1 mmol L^{-1}) in the same solution

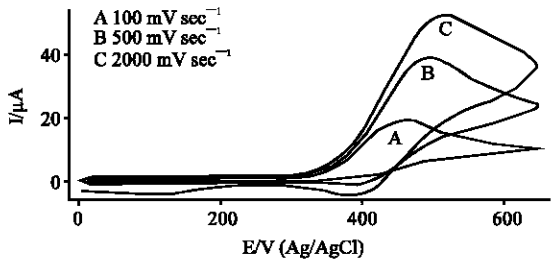

Fig. 5: Cyclic voltammograms of 2 mmol L^{-1} $[Ni(HL_2)_2]$ at different sweep rates

oxidative peaks (1, 3 and 2) at 25°C and at a sweep rate of 100 mV sec^{-1}. The two anodic processes (peak 3 and 2) together with the cathodic peaks (3'c and 3"c) are a result of the redox processes of H_2L_2 and H_2L_4 ligands. These signals are also observed in the CV of H_2L_2 and H_2L_4 under similar conditions. Not that the reverse scan at 1100 mV rises the appearance of peaks 3'c and 3"c indicating the association of these peaks and peak 3. The peaks 3 and 2 are tentatively attributed to the irreversible oxidation of the naphtyl group and NH group, respectively. The peak 1 may be assigned to the Ni(III)/Ni(II) redox couple.

On the other hand, we can note that on increasing the scan rate, for $[Ni(HL_2)_2]$ and $[Ni(HL_4)_2]$ at 2 mmol L^{-1}, from 100 to 2000 mV sec^{-1} (Fig. 5), the oxidation-reduction waves become more reversible-like. Probably this change is due to increase of scan rate and diffusion problems occur (Perez *et al*., 2005). This may be also due to the fact that the electron transfer reaction is followed by a chemical reaction. Note that the $[Ni(HL_1)_2]$ and $[Ni(HL_3)_2]$ complexes do not show the same behavior over the range of studied voltage sweep rates.

The peak current I_p, for oxidation peak 1 increased linearly with bulk solution concentration of $[Ni(HL_2)_2]$ over the concentration range 0.5-2 mmol L^{-1}. At concentrations higher than 2 mmol L^{-1} this increase was less than linear. Furthermore, it was shown that I_p increases linearly as a function of square root of the voltage sweep rate over the sweep rate range 100-2000 mV sec^{-1} at complex concentrations ≤2 mmol L^{-1}. At higher concentrations, the current increases with increasing square root of the voltage sweep rate, but was found to be non-linear. Moreover, the RDE study shows that for complex concentrations ≤2 mmol L^{-1}, the limiting current increases linearly with increasing electrode rotation speed. At higher complex concentrations, this increase was found to be of curved shape. These behaviors indicate that the peak 1 oxidation of $[Ni(HL_2)_2]$ is a diffusion controlled reaction over the entire range of voltage sweep rate studied at complex concentrations ≤2 mmol L^{-1}. At higher complex concentrations (>2 mmol L^{-1}), the current is governed by the rate of the charge transfer or of a chemical reaction. Moreover, it is possible to suggest that the formation of Ni(III) complexes undergoes an electron transfer followed by relatively fast chemical reaction, which probably results in the partial dissociation of the complexes.

On the other hand, a controlled-potential preparative electrolysis was carried out in a divided cell. An exhaustive oxidation of $[Ni(HL_2)_2]$ was performed at constant potential (500 mV). The anolyte was 20 mL of 0.5 mmol L^{-1} $[Ni(HL_2)_2]$ solution. A Pt electrode was used as the cathode. The result indicates that approximately 1 electron was transferred per molecule (n = 1.2). Since the peak currents I_{pa1} for all the complexes studied have approximately the same value, the number of electron involved in the oxidation of Ni(II) is 1 (for all the complexes). After exhaustive oxidation of $[Ni(HL_2)_2]$, the resulting solution was scanned from 0 to 1400 mV, the oxidized complex did not exhibit any oxidation signal Ni(II) → Ni(III) as shown in Fig. 6.

The electrochemical data of 2 mM nickel complexes studied are summarized in Table 3. A change in the formal potentials of the nickel(III)/nickel(II) couples, which occurs upon ligand substitution along this series is observed. A comparison of the redox potentials of the $[Ni(HL_3)_2]$ and $[Ni(HL_4)_2]$ complexes where both ligands H_2L_3 and H_2L_4 have the same set of donor atoms but differ in the size of central chelating agents shows that the nickel(III) complex $[Ni(HL_4)_2]$ is more stable thermodynamically, i.e., the Ni(III)/Ni(II) potential is lowered by 140 mV. The same result was obtained by comparing the redox potentials of $[Ni(HL_1)_2]$ and $[Ni(HL_2)_2]$. The Ni(III)/Ni(II) potential is, here, lowered by 150 mV. The lower oxidation potentials of $[Ni(HL_2)_2]$ and $[Ni(HL_4)_2]$ could be a result of the ability of naphtyl group to stabilize this oxidation state to a greater extend than phenyl group (Table 3). In fact, the substitution of the phenyl by naphtyl fragment causes an increase in aromatic character. This increase in aromatic character is enough to produce the observed negative shift in the formal potential. The electron density at the metal center is also enhanced as the aromatic character rises, thus facilitating its oxidation. In other respects, comparing the redox potentials of $[Ni(HL_2)_2]$ and $[Ni(HL_4)_2]$ on the one hand and those of $[Ni(HL_1)_2]$ and $[Ni(HL_3)_2]$ on the other hand shows a small negative shift of the Ni(III)/Ni(II) potential, indicating a weak effect of the CH_3 group.

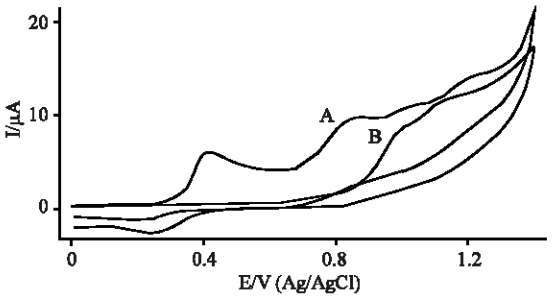

Fig. 6: Cyclic voltammograms of 0.5 mmol L^{-1} $[Ni(HL_2)_2]$ before (A) and after (B) exhaustive oxidation

Table 3: Cyclic voltammetric data of the studied complexes*

	Ep (V)				
Complex	Ep_a (1)	Ep_a (2)	Ep_a (3)	Ep_c (3'c)	Ep_c (3"c)
$[Ni(HL_1)_2]$	0.58	1.22	-	-	-
$[Ni(HL_2)_2]$	0.43	1.28	0.95	0.81	0.23
$[Ni(HL_3)_2]$	0.55	1.23	-	-	-
$[Ni(HL_4)_2]$	0.41	1.25	0.94	0.81	0.23

*c = 2 mmol L^{-1} in DMSO solution (0.1 mol L^{-1} $N(Et)_4ClO_4$), E values (V versus Ag/AgCl/3 mol L^{-1} KCl), Scan rate 100 mV sec^{-1}, E_{pa} and E_{pc} are the anodic and cathodic peak potentials, respectively

CONCLUSION

In this study, we could synthesize Ni(II) hydrazone derivatives complexes containing nitrogen and oxygen donor atoms. The structure determinations of ligands and their complexes were established by elemental analysis, magnetic moments and UV, IR and ^{1}H-NMR spectra. In all complexes, the geometry around the nickel(II) ions is square planar. It was suggested that the ligands exist in two forms (free and hydrogen-bonded). Electrochemistry data show that the Ni(II) complexes displayed Ni(III)/Ni(II) couples irreversible waves and that the substitution of the phenyl by naphtyl fragments causes a large enough increase in aromatic character to produce a negative shift in the formal potential.

REFERENCES

Armstrong, C.M., P.V. Bernhardt, P. Chin and D.R. Richardson, 2003. Structural variations and formation constants of first-row transition metal complexes of biologically active aroylhydrazones. Eur. J. Inorg. Chem., 6: 1145-1156.

Bakir, M., I. Hassan, T. Johnson, O. Brown, O. Green, C. Gyles and M.D. Coley, 2004. X-ray crystallographic, electrochemical and spectroscopic properties of 2-pyridinio 2-pyridyl ketone phenyl hydrazonechloride hydrate. J. Mol. Struct., 688: 219-222.

Becker, R.S. and F. Chagneau, 1992. Comprehensive investigation of the photophysics, photochemistry and kinetics of a wide variety of photochromic hydrazones in various solvents. J. Am. Chem. Soc., 114: 1373-1381.

Bellamy, L.J., 1958. The infrared Spectra of Complex Molecules. 1st Edn., Wiley, New York.

Bour, J.J., P.J.M.W.L. Birker and J.J. Steggerda, 1971. Copper(III) and nickel(III) complexes of biuret and oxamide. Inorg. Chem., 10: 1202-1205.

Bulanov, O., B.S. Luk'yanov, V.A. Kogan, N.V. Stankevich and V.V. Lukov, 2002. Photo and thermochromic spirans. New metal chelates based on azomethines and hydrazones containing a spiropyran fragment. Russ. J. Coord. Chem., 28: 46-49.

Bullock, J.I. and H.A. Tajmir-Riahi, 1978. Schiff-base complexes of the lanthanoids and actinoids. Part 1. Lanthanoid(III) halide complexes with the un-ionised form of NN'-ethyl-enebis (salicylideneimine) and related bases. J. Chem. Soc., Dalton Trans., 1: 36-39.

Cervera, B., J.L. Sanz, M.J. Ilbanez, G. Vila and F.L. Loret *et al*., 1998. Stabilization of copper(III) complexes by substituted oxamate ligands. J. Chem. Soc., Dalton Trans., 5: 781-790.

Chandra, S. and R. Kumar, 2004. Synthesis and spectral studies on mononuclear complexes of chromium (III) and manganese(II) with 12-membered tetradentate N_2O_2, N_2S_2 and N_4 donor macrocyclic ligands. Trans. Mater. Chem., 29: 269-275.

Chandra, S. and R. Kumar, 2005. Electronic, cyclic voltammetry, IR and EPR spectral studies of copper(II) complexes with 12-membered N_4, N_2O_2 and N_2S_2 donor macrocyclic ligands. Spectrochim. Acta Part A, 65: 437-446.

Chandra, S., L.K. Gupta and Sangeetika, 2005. Spectroscopic, cyclic voltammetric and biological studies of transition metal complexes with mixed nitrogen-sulphur (NS) donor macrocyclic ligand derived from thiosemicarbazide. Spectrochim. Acta Part A, 62: 453-460.

Chandra, S., R. Kumar and R. Singh, 2006. Nickel(II) complexes with different chromospheres containing macrocyclic ligands: Spectroscopic and electrochemical studies. Spectrochim. Acta Part A, 65: 215-220.

Feigl, R., 1982. Spot Test in Organic Analysis. 6th Edn., Elsevier, Amsterdam, pp: 470-483. ISBN-10: 0444409297.

Ferraro, J.R., 1971. Low Frequency Vibrations of Inorganic and Coordination Compounds. 1st Edn., Plenum Press, New York. pp: 102 and 223. ISBN-0-306-30453-8.

Geary, W.J., 1971. The use of conductivity measurements in organic solvents for the characterization of coordination compounds. Coord. Chem. Revs., 7: 81-122.

Hadjoudis, E. and I.M. Mavridis, 2004. Photochromism and thermochromism of Schiff bases in the solid state: Structural aspects. Chem. Soc. Revs., 33: 579-588.

Jacques, P., 1984. Substituent effects on the tautomerism and photochromism exhibited by a series of hydroxyazo cationic dyes for polyester fibres. Dyes Pigments, 5: 351-370.

Larabi, L., Y. Harek, A. Reguig and M.M. Mostafa, 2003. Synthesis, structural study and electrochemical properties of copper(II) complexes derived from benzene- and p-toluenesulphonylhydrazones. J. Serb. Chem. Soc., 68: 85-95.

Lever, A.B.P., 1968. Inorganic Electronic Spectroscopy. 2nd Edn., Elsevier, Amsterdam, pp: 534-544. ISBN-0-444-42389-3.

Margerum, D.W., K.L. Chellappa, F.P. Bossu and G.L. Burce, 1975. Characterization of a readily accessible copper(III)-peptide complex. J. Am. Chem. Soc., 97: 6894-6896.

Nicholson, R.S. and I. Shain, 1964. Theory of stationary electrode polarography single scan and cyclic methods applied to reversible, irreversible and kinetic systems. Anal. Chem., 36: 706-723.

Perez, F.R., L. Basaez, J. Belmar and P. Vanisek, 2005. Cyclic voltammetry of 1-(n-hexyl)-3-methyl-5-pyrazolone-based enamines and their chloromanganese(III) and nitridomanganese(I) complexes. J. Chil. Chem. Soc., 50: 87-97.

Rao, C.N.R., 1975. Ultraviolet and Visible Spectroscopy. 3rd Edn., Plenum Press, New York, ISBN-0-408-70624-4, pp: 33-48.

Razmi-Nerbin, H. and M.H. Pournaghi-Azar, 2002. Nickel pentacyanonitrosylferrate film modified aluminum electrode for electrocatalytic oxidation of hydrazine. J. Solid State Electrochem., 6: 126-133.

Ruiz, R., C. Surville-Barland, A. Aukauloo, E. Anxolabehere-Mallart and Y. Journaux *et al.*, 1997. Stabilization of copper(III) complexes by disubstituted oxamides and related ligands. J. Chem. Soc., Dalton Trans., 5: 745-751.

Sacconi, L., 1966. Four, five and six coordinated complexes of 3D metals with substituted salicylaldimines. Coord. Chem. Rev., 1: 192-204.

Schmidt, I. and P.J. Chmielewski, 2003. Nickel(II) complexes of 21-C-alkylated invertedporphyrins: Synthesis, protonation and redox properties. Inorg. Chem., 42: 5579-5593.

Schmitt, J.L., A.M. Stadler, N. Kyritsakas and J.M. Lehn, 2003. Helicity-encoded molecular strands: Efficient access by the hydrazone route and structural features. Helv. Chim. Acta, 86: 1598-1624.

Vogel, A.I., 1989. Text Book of Practical Organic Chemistry. 5th Edn., Longnann, New York, ISBN-0-582-46236-3, pp: 873-878.

Wong, J.L. and F.N. Bruscato, 1968. Photochromism of quinolylhydrazones. Tetrahedron Lett., 9: 4593-4596.

Zady, M.F., F.N. Bruscato and J.L. Wong, 1975. Structural criteria for hydrazone photochromism in solution. J. Chem. Soc., Perkin Trans., 1: 2036-2039.